DALTON
FULL PAPER

Lanthanide triple helical complexes with a chiral ligand derived from 2,6-pyridinedicarboxylic acid †

Gilles Muller,[a] Boris Schmidt,[b,c] Jan Jiricek,[c] Gérard Hopfgartner,[d] James P. Riehl,[e] Jean-Claude G. Bünzli *[a] and Claude Piguet[f]

[a] *Institute of Inorganic and Analytical Chemistry, BCH, University of Lausanne, CH-1015 Lausanne, Switzerland. E-mail: jean-claude.bunzli@icma.unil.ch*
[b] *Novartis Pharma AG, Nervous System, WKL 136.5.82, CH-4002 Basel, Switzerland*
[c] *Department of Organic Chemistry, University of Hannover, Schneiderberg 1b, D-30167 Hannover, Germany*
[d] *F. Hoffmann-La Roche Ltd, Pharmaceuticals Division, PRNS 68/142, CH-4070 Basel, Switzerland*
[e] *Department of Chemistry, University of Minnesota Duluth, Minnesota, 55812-2496, USA*
[f] *Department of Inorganic, Analytical and Applied Chemistry, University of Geneva, 30 quai E. Ansermet, CH-1211 Geneva 4, Switzerland*

Received 26th March 2001, Accepted 18th June 2001
First published as an Advance Article on the web 22nd August 2001

The ligand 3-[2,6-bis(diethylcarbamoyl)pyridine-4-yl]-*N*-(*tert*-butoxycarbonyl)alanine methyl ester (L^4) bearing a chiral group in the 4-position of the pyridine ring has been synthesised and its interaction with trivalent lanthanide ions studied. L^4 yields stable $[Ln(L^4)_3]^{3+}$ complexes in acetonitrile, with $\log\beta_3$ in the range 19–20. The specific rotary dispersion of the complexes is about ten times as large as that of the ligand alone, consistent with triple helical structures in solution. NMR data show the presence of only one time-averaged species in acetonitrile solution with a trigonal symmetry, that is, the helical P $\rightleftharpoons$ M interconversion is fast on the NMR time scale. Circularly polarised luminescence on the Eu and Tb triple helical complexes displays weak effects, pointing to only a small diastereomeric excess in solution. High resolution luminescence spectra of the Eu complex in the solid state reveal a local symmetry derived from a trigonal arrangement around the metal ion and the long $^5D_0$ lifetime (1.58 ms) is indicative of the absence of water molecules bound in the inner co-ordination sphere. Energy transfer processes in the luminescent Eu and Tb triple helical complexes are discussed.

Introduction

The considerable interest in lanthanide co-ordination chemistry, which has steadily risen during the last two decades, is essentially motivated by applications in biology and medicine, mainly for analysis[1] and diagnosis purposes[2] but, also, for therapeutic uses.[3] One challenge pertaining to the design of functional lanthanide-containing co-ordination compounds lies in the need for a precise control of the Ln(III) inner co-ordination sphere: these ions present non-directional bonding and large and variable co-ordination numbers.[4] Various strategies have been developed to master this difficulty, for instance the encapsulation of the spherical Ln(III) ions into pre-organised macrocyclic ligands or into cavities built from pre-disposed molecules or through the self-assembly of carefully tailored multidentate ligands and podands.[5,6] In the latter strategy a finer recognition can be achieved if weak non-covalent inter-strand interactions are used to stabilise the functional edifices. Working along these lines, we have shown that bis(benzimidazole)pyridines (bzimpy, Scheme 1) are versatile tridentate aromatic donors acting as building blocks for various monotopic and ditopic receptors aimed at designing triple helical monometallic and bimetallic (4f–4f and 3d–4f) functional molecular edifices with light-converting or spin-crossover capability,[5,7] or as candidates for rod-like extended materials.[8]

† Electronic supplementary information (ESI) available: further analysis of the structures $Ln(ClO_4)_3{\cdot}xH_2O$ and $[Ln(L^4)_3]^{3+}$. See http://www.rsc.org/suppdata/dt/b1/b102728j/

Dipicolinic acid (H_2dipic) and its derivatives are also good candidates for the design of triple-stranded Ln(III) building blocks with interesting luminescence properties. For instance, the optically-active $[Ln(dipic)_3]^{3-}$ complexes are strongly luminescent in water and circularly polarised luminescence shows that the enantiomeric excess in the ground state can be modulated by the addition of chiral sugars.[9] On the other hand, we have shown that the weakly stable $[Ln(L^2)_3]^{3+}$ complexes exist as a mixture of rapidly interconverting P $\rightleftharpoons$ M conformers with Ln = Eu, Tb displaying fair quantum yields in acetonitrile, while $[Ln(L^1)_3]^{3+}$ complexes are more stable but less luminescent.[10,11] The triple helical complexes are inherently chiral but they usually appear as racemic mixtures both in the solid state and in solution (often as fast interconverting isomers). However, a small excess of one helical enantiomer can be induced in the excited state *via* the use of circularly polarised excitation light.[12] Related helical induction in the ground state requires diastereomeric resolution and we recently have introduced a chiral substituent in the R^2 position of bzimpy to give L*. However, the bulky neopentyl substituent precludes the helical wrapping of the third ligand, resulting in a very low stability of the $[Ln(L^*)_3]^{3+}$ complexes.[13] In this paper we turn to the substituted pyridine-2,6-dicarboxamide ligand L^4, where a chiral group is grafted onto the 4-position of the pyridine ring, which should lead to (i) less steric hindrance and (ii) easier helical wrapping of the three ligand strands around the Ln(III) ions, thus providing pairs of diastereoisomers for the triple helical complexes $[Ln(L^4)_3]^{3+}$.

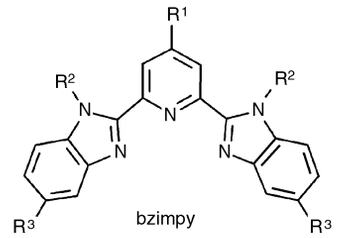

$R^1 = R^3 = H$, R^2 = neopentyl: L*

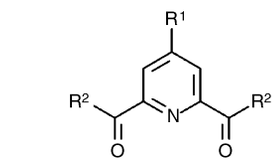

R^1 = H	R^2 = OH	H_2dipic
H	NEt_2	L^1
H	OEt	L^2
$C_2H_4CO_2CMe_3$	NEt_2	L^3

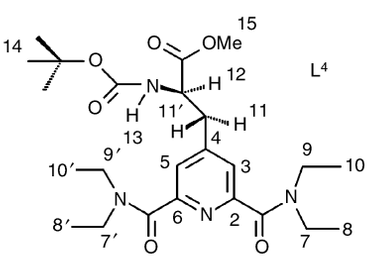

Scheme 1

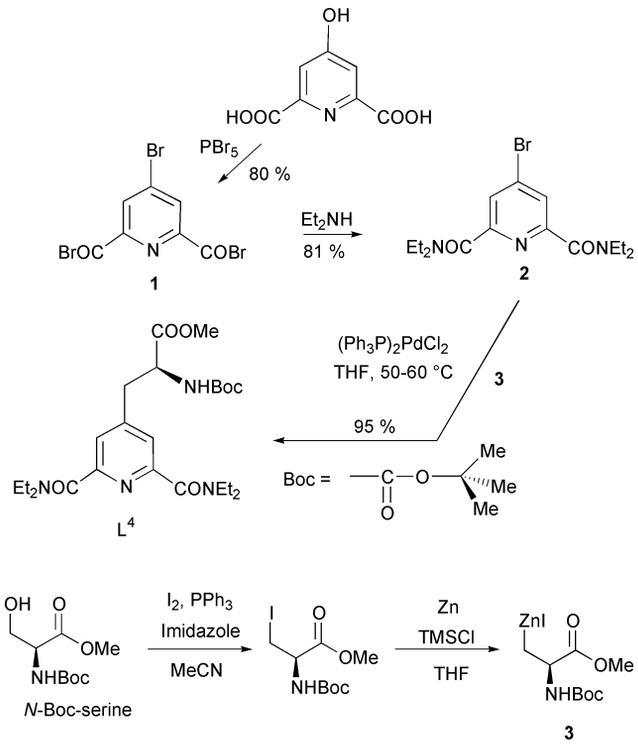

Scheme 2

Results and discussion

Synthesis and characterisation of the ligand and its complexes

Ligand L^4 was synthesised from 4-bromo-*N*,*N*,*N*′,*N*′-tetraethylpyridine-2,6-dicarboxamide **2** *via* a palladium mediated reaction with Jackson's zinc reagent **3** (Scheme 2). Despite previous discouraging reports on the activity of $(Ph_3P)_2PdCl_2$,[14,15] this catalyst proved to be better than $(PPh_3)_4Pd$ or $Pd(OAc)_2$[16] and gave L^4 in excellent yield (95%). Takalo's approach[17,18] was used to prepare **2** by treatment of chelidamic acid with phosphorous pentabromide and hydrolysis of the intermediate acid bromide with diethylamine. Jackson's zinc reagent **3** was synthesised from *N*-Boc-serine[14,15] using a single-step procedure to get iodoalaninemethyl ester by a combination of I_2/PPh_3/imidazole reagents. This method gave a better yield (61%)[19] and made isolation of the final product easier than with the originally proposed method.[14] This was then followed by a Knochel's zinc activation reaction[20] ($BrCH_2CH_2Br$, trimethylsilylchloride) which was revealed to be the method of choice, provided that the recommended zinc dust was replaced by zinc turnings to allow reagent transfer *via* cannulation. Slow reaction rates and excess of zinc have to be avoided to prevent palladium(0) precipitation and decomposition of iodoalanine into di-dehydroalanine. The best results were obtained with zinc amounts reduced to one third of the reported reaction conditions.[20] Other methods of zinc activation such as ultrasound, CuCN, $HgCl_2$, DMA or Rieke™ zinc led to inferior results. The replacement of THF by DMF, DMA, toluene or benzene or combinations thereof was also unsuccessful.

The specific rotary dispersion of L^4 in anhydrous and degassed acetonitrile, $[\alpha]_D^{25} = -3.5 \pm 0.4$ deg dm^2 mol^{-1}, confirms the chirality arising from the asymmetric carbon. ^{1}H- and ^{13}C-NMR spectra in the same solvent, including COSY, DEPT-135, HSQC and NOE experiments, clearly point to L^4 having a *trans–trans* conformation of the terdentate binding units in agreement with that predicted by gas-phase molecular mechanics calculations using the AM1 package (Fig. S1†).[21] At room temperature, the ^{1}H- and ^{13}C-NMR spectra display 11 and 13 signals, respectively, pointing to a local two-fold symmetry for the pyridine dicarboxamide portion of the molecule: $X^{3,5}$, $X^{7,7'}$, $X^{8,8'}$, $X^{9,9'}$ and $X^{10,10'}$ (X = H, C) and $C^{2,6}$ give rise to only one signal each.

The 1 : 3 complexes were obtained in 70–80% yield by adding L^4 dissolved in dichloromethane to solutions of lanthanide perchlorates in a mixture of CH_3CN and CH_2Cl_2. Complexation is evidenced by the shift of the ν_{CO} vibration to lower energy ($\Delta\nu = -29$ cm^{-1} for La to -22 cm^{-1} for Lu), reflecting a lowering in the electron density of the carbonyl double bond and/or a larger reduced mass associated with the complexation to Ln^{III}. All perchlorate ions are ionic, so that the complexes are most probably 9-co-ordinate. Single crystals for X-ray structure determination could not be obtained.

Interaction between L^4 and Ln(III) ions

To quantify this interaction, we first measured ES-MS spectra in order to identify the various species in solution. Solutions of L^4 (10^{-4} M in anhydrous acetonitrile) were titrated with $Ln(ClO_4)_3 \cdot xH_2O$ (x = 0.3–0.6) at 298 K for ratios $R = [L^4]_t/[Ln(III)]_t = 0$–3. The data show that the Boc substituent is easily split (FW = 101 Da) in the gas-phase, giving rise to a primary amine $L^{4'}$. As a result, the spectra reflect the presence of $[Ln(L^4)_n]^{3+}$ (n = 1–4), $[Ln(L^{4'})_m]^{3+}$ (m = 2–4) and $[Ln(L^4)_p(L^{4'})_q]^{3+}$ ($p = 1$, q = 1–2; $p = 2$, $q = 1$) species, some of them with solvation molecules and/or in the form of perchlorate adducts. All the identified species are listed in Table S1†. These data clearly support the successive formation of 1 : 1, 1 : 2 and 1 : 3 species, as well as of a species with four ligands. Such species have been observed for similar systems and were assigned to outer-sphere association of a fourth ligand with a 1 : 3 edifice.[10] It is noteworthy that the proportion of the various species is dependent upon the ionic radius of the metal ion (Table 1). For $R = 3$, the 1 : 3 complex is the most abundant one for the three investigated ions, while solutions containing the larger La(III) ions contain sizeable amounts of the 1 : 4 species, in line with the explanation given above. On the other hand, the perchlorato adducts $[Ln(L^4)_3(ClO_4)]^{2+}$ form more easily with cations which

Table 1 Relative intensities of the ES-MS peaks for solutions with $[L^4]_t/[Ln(III)]_t = 3$ (CH_3CN, 298 K)

Species	La	Eu	Lu	Species	La	Eu	Lu
$[Ln(L^4)_2]^{3+}$	55.6	4.7	0.0	$[Ln(L^4)(L^{4\prime})]^{3+}$	14.8	0.0	0.0
$[Ln(L^4)_3]^{3+}$	100	100	100	$[Ln(L^4)(L^{4\prime})_2]^{3+}$	0.0	19.1	27.0
$[Ln(L^4)_4]^{3+}$	40.7	8.8	10.8	$[Ln(L^4)_2(L^{4\prime})]^{3+}$	16.7	0.0	0.0
$[Ln(L^4)_2(ClO_4)]^{2+}$	7.4	0.0	1.3	$[Ln(L^4)_2(L^{4\prime})_2]^{3+}$	5.9	0.0	0.0
$[Ln(L^4)_3(ClO_4)]^{2+}$	7.4	35.3	37.8	$[Ln(L^4)(L^{4\prime})(ClO_4)]^{2+}$	0.0	0.0	8.1
$[Ln(L^4)_4(ClO_4)]^{2+}$	1.8	1.5	0.0	$[Ln(L^4)(L^{4\prime})_2(ClO_4)]^{2+}$	0.0	6.5	0.0

Table 2 Cumulative stability constants $\log\beta_n$ (298 K, ± 2σ) for $[Ln(L^i)_n]^{3+}$ species (i = 1, 3, 4; n = 1–3) as determined under anhydrous conditions in acetonitrile by spectrophotometry

Ligand	Ln	$\log\beta_1$	$\log\beta_2$	$\log\beta_3$
L^3	La	7.4 ± 0.4	14.0 ± 0.5	19.0 ± 0.5
	Eu	8.2 ± 0.4	14.5 ± 0.5	19.8 ± 0.5
	Lu	8.7 ± 0.4	15.3 ± 0.5	20.3 ± 0.5
L^4	La	7.4 ± 0.4	13.9 ± 0.5	19.0 ± 0.5
	Eu	8.2 ± 0.4	14.6 ± 0.5	19.7 ± 0.5
	Lu	8.7 ± 0.4	15.2 ± 0.5	20.5 ± 0.5
L^1 [a]	La	7.4 ± 0.3	14.8 ± 0.3	21.0 ± 0.3
	Eu	8.3 ± 0.3	15.3 ± 0.3	22.3 ± 0.3
	Lu	8.1 ± 0.3	15.2 ± 0.3	22.9 ± 0.3

[a] From ref. 11.

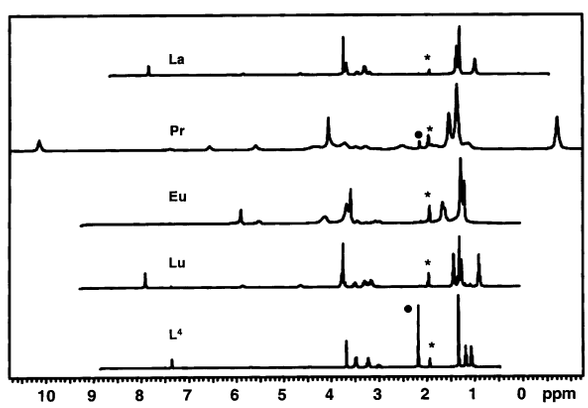

Fig. 1 ^{1}H-NMR spectra of L^4 and $[Ln(L^4)_3]^{3+}$ (5×10^{-3} M in CD_3CN at 298 K); asterisk and small circle (•) correspond to signals from the solvent and water, respectively.

have a larger charge density (Eu, Lu) than with La. This speciation has been confirmed in solution by monitoring the titration of L^4 with La(III) by ^{1}H-NMR: the spectra of the three inner-sphere complexes could be identified and when $R = 3$, the 1 : 3 species is the main complex in solution (>92%, see Fig. S2†). The apparent easy formation of the 1 : 3 species contrasts with what was observed with L* and points to the substitution in the R^1 position of the central pyridine not preventing the formation of the helical complexes.

To quantify further the Ln(III)–L^4 interaction, we performed spectrophotometric titrations of both L^3 and L^4 against $Ln(Otf)_3$ (Ln = La, Eu, Lu; Otf = trifluoromethanesulfonate) in MeCN under anhydrous conditions ($[H_2O]$ < 30 ppm). The ligand L^3 is an achiral analogue of L^4. Factor analysis indicated the presence of three or four absorbing molecules and the data were fitted by a least-squares procedure using either set (1)–(3) of the following equilibria, where solvation and anion co-ordination has been omitted, or a model including $[Ln(L^i)_4]^{3+}$ chosen since this species was found in the ES-MS spectra. Increasing the number of complex species however did not improve the fit, in line with the postulated outer-sphere nature of this 1 : 4 species.

$$Ln^{3+} + L^i \rightleftharpoons [Ln(L^i)]^{3+} \quad \log\beta_1 \qquad (1)$$

$$Ln^{3+} + 2\,L^i \rightleftharpoons [Ln(L^i)_2]^{3+} \quad \log\beta_2 \qquad (2)$$

$$Ln^{3+} + 3\,L^i \rightleftharpoons [Ln(L^i)_3]^{3+} \quad \log\beta_3 \qquad (3)$$

Electronic spectra of the three complexes were correlated, which rendered the fitting process difficult and generated relatively large uncertainties in the $\log\beta_i$ values. The results are reported in Table 2, along with comparative data for L^1. Stability constants for L^3 and L^4 are identical, within experimental errors, indicating that the introduction of the NH Boc on C^{12} does not affect complex formation. If $\log\beta_1$ and $\log\beta_2$ are the same, within experimental errors, for the three ligands $L^{1,3,4}$, a different pattern is observed for $\log\beta_3$. The triple helical species with ligands L^3 and L^4 are somewhat less stable than those with L^1, the difference increasing from La to Lu, as shown by $\Delta\log\beta_3(L^1 - L^i) = 2$ for La and 2.4–2.6 for Lu (i = 3, 4). Therefore, the poor electron attracting group in R^1 has a minor destabilising effect as measured for Ln = La, and its steric hindrance, which is comparable in both L^3 and L^4, destabilises somewhat the complexes with the smaller lanthanide ions.

Solution structure and dynamic behaviour of the $[Ln(L^4)_3]^{3+}$ complexes

The ^{1}H-NMR spectra of the 1 : 3 complexes are displayed in Fig. 1 and chemical shifts are reported in Table 3. At room temperature, these spectra point to a trigonal symmetry of the complexes with equivalent ligand strands. The chemical shifts induced by the complexation are in line with those reported for complexes with L^1 and, together with NOE effects observed between H^3–H^9 are characteristic of a meridional co-ordination of the tridentate binding unit of each ligand strand. Moreover, the large downfield shifts of the signals of $H^{3,5}$ and $C^{3,5}$ indicate co-ordination of the pyridine N atom to the Ln(III) ions. Analysing in more detail the spectra of the diamagnetic complexes with La and Lu, we find substantial differences for the protons of the *N*-ethyl substituents and of the Boc group. For instance, H^7 and H^9 appear as a single broadened quadruplet (4H) for La while they give rise to two resolved quadruplets with similar intensities (2H) for Lu. An immediate conclusion is that the rotation around the C–N amide bond is slower in the Lu structure, as previously observed for $[Ln(L^1)_3]^{3+}$ and ascribed to the larger charge density of Lu(III) which hinders the amide rotation process by reducing the electron density of the co-ordinated carbonyl group.[10] Moreover, the equivalence of the geminal protons of the methylene probes implies that fast P $\rightleftharpoons$ M helical interconversion occurs at room temperature on the NMR time scale along the complete lanthanide series. Differences appear also for the H^{14} protons, one signal being observed for La and three for Lu; this is also indicative of a slowing down of the rotation process of the Boc group in the case of the smaller lanthanide ion.

A variable temperature study of the Lu solution (234–340 K, Fig. S3†) shows that the H^{14} protons appear as two singlets of approximately the same intensity at elevated temperature while they give rise to at least 6–7 signals at 242 K, two of them being substantially more intense than the others. The hindered rotation about the OC–N bond of the carbamate groups in

Table 3 ^{1}H and ^{13}C chemical shifts (ppm) for L^4 and its $[Ln(L^4)_3]^{3+}$ complexes with Ln = La, Pr, Eu and Lu (CD_3CN, 5×10^{-3} M, 298 K)

	$H^{3,5}$	$H^{7,7'}$	H^{8}	$H^{9,9'}$	H^{10}	$H^{11,11'}$	H^{12}	H^{13}	H^{14}	H^{15}
L^4	7.35	3.23	1.07	3.49	1.19	3.00, 3.22	4.46	5.70	1.34	3.68
La	7.84	3.29	0.98	3.68	1.37	3.19, 3.45	4.64	5.84	1.30	3.74
Pr	10.14	1.80, 2.49	−0.74	3.70, 4.30	1.52	3.26, 3.46	5.58	6.55	1.35	4.04
Eu	5.87	3.67, 4.15	1.27	3.67	1.68	3.01, 3.44	4.15	5.52	1.21	3.59
Lu	7.90	3.12, 3.29	0.89	3.74	1.42	3.20, 3.49	4.62	5.87	1.25 1.30 1.34	3.74

	$C^{3,5}$	C^{7}	C^{8}	C^{9}	C^{10}	C^{11}	C^{12}	C^{14}	C^{15}	$C^{quat.}$
L^4	123.20	39.48	12.14	42.85	13.59	36.45	53.82	27.44	51.97	149.05, 154.31, 167.77, 171.80
La	127.47	42.45	11.43	44.68	13.35	37.01	53.33	27.48	52.32	149.77, 153.62, 169.28, 171.27
Pr	142.60	42.41	9.49	46.07	12.84	39.81	52.99	27.48	52.67	152.66, 157.77, 169.28, 171.89
Eu	95.25	41.79	12.80	42.48	14.70	33.33	54.87	27.39	52.18	143.62, 162.68, 163.23, 171.03
Lu	128.07	43.52	11.45	44.85	13.35	36.83	53.33	27.39	52.35	147.77, 153.53, 168.30, 171.35

$[Ln(L^4)_3]^{3+}$ provides four different conformers for each diastereoisomer, defined by the *cis* or *trans* position of the H^{13} atom with respect to the neighbouring O carbonyl atom. For a given diastereoisomer, we predict that H^{14} produces one signal in the ^{1}H-NMR spectrum for the *cis–cis–cis* (symmetry C_3), one signal for the *trans–trans–trans* (symmetry C_3), three signals for the *cis–trans–cis* (symmetry C_1) and three signals for the *trans–trans–cis* conformer (symmetry C_1) in the statistical ratio 1 : 3 : 3 : 1 if no steric or electronic constraints are present. Therefore the H^{14} protons can theoretically generate 8 signals for each diastereoisomer, that is a total of 16 signals if both diastereoisomers are present. However, in our case, examination of the signals arising from the other nuclei (H and C) clearly points to the solutions containing one major diastereoisomer only, as several other studies on complexes between d- and f-transition ions and potentially chiral ligands have shown.[22–24] We were however unable to assign the observed signals and to exploit quantitatively the spectral changes as a function of temperature. The rotation of the *N,N′*-diethylamide and Boc groups is also seen in the variable temperature spectra of the Pr and Eu complexes. At 332 K, proton H^{14} gives rise to one signal only whereas 5 peaks are observed at 234 K. However two of the conformers have much larger populations than the other ones, as demonstrated by the ^{13}C-NMR spectra which evidence the splitting of the C^{14} signal at 298 K into two components at 244 K (Fig. S4†). In the case of Pr, the rotation process is considerably slowed down with respect to La, and we were able to determine the kinetic parameters for the interconversion between the two major conformers (275–298 K) using the Eyring equation: $\Delta G^{\ddagger}$ = 57.7 ± 0.6 kJ mol^{-1}, $\Delta H^{\ddagger}$ = 45.8 ± 0.3 kJ mol^{-1}, $\Delta S^{\ddagger}$ = −40.0 ± 1.0 J mol^{-1} K^{-1}, and k(298 K) = 479 ± 11 s^{-1}. These parameters correspond to the most energetic process going on in solution. For T < 275 K, the spectra point to the presence of other conformers the interconversion of which is faster. Although the introduction of the chiral group in R^1 together with the use of an amide-type spacer between the asymmetric carbon and the Boc group result in complications in the ^{1}H-NMR spectra, the solution behaviour of the $[Ln(L^4)_3]^{3+}$ complexes is very similar to that previously reported for $[Ln(L^1)_3]^{3+}$ [11] except for the increased rate of the dynamic process involving P ⟾ M helical interconversion in $[Ln(L^4)_3]^{3+}$.

To assess whether or not the ligand strands are helically wrapped around the metal ion, we measured the specific rotary dispersion of solutions of the $[Ln(L^4)_3]^{3+}$ complexes (10^{-3} M in anhydrous acetonitrile). This experiment occurs on a time scale where P ⟾ M helical interconversion is blocked in $[Ln(L^4)_3]^{3+}$. The specific rotary dispersion amounts to $[a]_D^{25}$ = −35, −30, −28, and −31 deg dm^2 mol^{-1} for La, Eu, Tb, and Lu, respectively and is about ten times larger than the rotary dispersion measured for the ligand alone. Therefore, there is no doubt that $[a]_D^{25}$ contains a large structural contribution, pointing to the formation of triple helical complexes in solution. As a comparison, $[a]_D^{25}$ is approximately equal to one or two times the rotary dispersion of the ligand in 1 : 1 and 1 : 2 complexes with L*, for which no (1 : 1) or little, (1 : 2) structural contribution is expected.[12] Circularly polarised luminescence (CPL) spectra for the Eu and Tb complexes are reported in Fig. 2. They display very small ΔI values for the $^{5}D_0 \overset{257}{\rightarrow} {}^{7}F_1$(Eu) and $^{5}D_4 \overset{257}{\rightarrow} {}^{7}F_5$(Tb) transitions. The CPL spectrum of the Eu complex depends upon the polarisation of the excitation light, indicating the presence of two species in solution,[24] in line with the speciation that can be calculated from the stability constants: 10^{-3} M solutions contain 92% of the 1 : 3 species and 8% of the 1 : 2 species, which is expected to generate a smaller chiral effect. The CPL spectrum of the $^{5}D_4 \longrightarrow {}^{7}F_5$(Tb) transition displays several peaks corresponding to crystal-field splitting of the electronic levels.[24] The calculated g_{lum} factor amounts to 0.02 only, a value substantially smaller than those reported for chiral complexes with trigonal symmetry.[23] These CPL data are consistent with the presence of only a small excess of one diastereoisomer in solution on the short time scale of optical measurements.

Photophysical properties

The electronic spectrum of the ligand in solution displays an intense band centred around 51 000 cm^{-1} corresponding to a transition mainly centred on the carbonyl groups. Its intensity considerably increases upon complexation, indicating a strong interaction between the carbonyl functions and the metal ions (Table 4, Fig. S5†). In addition, two weak and broad bands are seen around 41 150 and 37 460 cm^{-1}, assigned to transitions mainly centred on the pyridine groups.[11] Upon complexation, the energy gap between these two transitions increases from 3700 cm^{-1} in the free ligand to *ca.* 6500 cm^{-1} in the complexes. In the solid state, the gap becomes larger, being *ca.* 10 000 cm^{-1}. No significant emission is detected upon irradiation of L^4 in the UV region (solution and solid state), pointing to the existence of efficient non-radiative de-activation pathways in the free ligand. On the other hand, ligand emission is observed for the complexes. Fluorescence from a short-lived $^{1}\pi\pi^*$ state occurs for all complexes while ligand phosphorescence from a long-lived $^{3}\pi\pi^*$ state is seen for the La and Lu complexes only, an efficient $^{3}\pi\pi^*$-to-Ln energy transfer process taking place for Eu and Tb complexes and resulting in metal-centred emission exclusively (Fig. 3). The 0-phonon transitions observed for emissions from both the singlet and triplet states are slightly shifted toward lower energy when going from La to Lu, consistent with the larger charge density of the heavier Ln(III) ion. The

Table 4 Ligand-centred absorptions in acetonitrile and in the solid state (293 K), ligand-centred singlet- and triplet-state energies as determined from emission spectra of the solids (77 K) and of solutions (10^{-3} M in acetonitrile, 293 K) for the ligand L^4 and its triple helical complexes $[Ln(L^4)_3]^{3+}$ [a]

	E/cm^{-1} [b]		$E(^1\pi\pi^*)$/cm^{-1}		$E(^3\pi\pi^*)$/cm^{-1}
Compound	Solution [c]	Solid state	Solution	Solid state [d]	Solid state [d]
L^4	50010 (4.36)		[e]	[e]	[e]
	41150 (3.71)	40330 sh			
	37460 (3.65)	36900			
$[La(L^4)_3]^{3+}$	49750 (4.92)	45870 sh			
	42320 (4.49) sh	36360		*31990*	*25190*
	35820 (4.26)	26110	23150	25575	18345
	35060 (4.23) sh				
$[Eu(L^4)_3]^{3+}$	49140 (4.91)	43860 sh		[f]	[f]
	41270 (4.50) sh	37175			
	35850 (4.31)	25445	24180		
	34850 (4.26) sh				
$[Tb(L^4)_3]^{3+}$	49140 (4.89)	46510 sh		[f]	[f]
	42220 (4.45) sh	35970			
	35630 (4.25)	25445	23140		
	34940 (4.24) sh				
$[Lu(L^4)_3]^{3+}$	49260 (4.86)	44385 sh			
	42000 (4.46) sh	35000		*30745*	*23200*
	35760 (4.21)	25000	24210	25760	17610
	34900 (4.17) sh				

[a] sh = shoulder. [b] Ligand-centred transitions. [c] At the concentration used, 92% of the metal ions are in the form of the 1 : 3 complex and 8% in the form of the 1 : 2 complex; log ε values are given in parentheses. [d] The 0-phonon transition is given in italics for frozen solutions in acetonitrile. [e] Too weak to be observed. [f] Not observed because of the L^4-to-Ln energy transfer process.

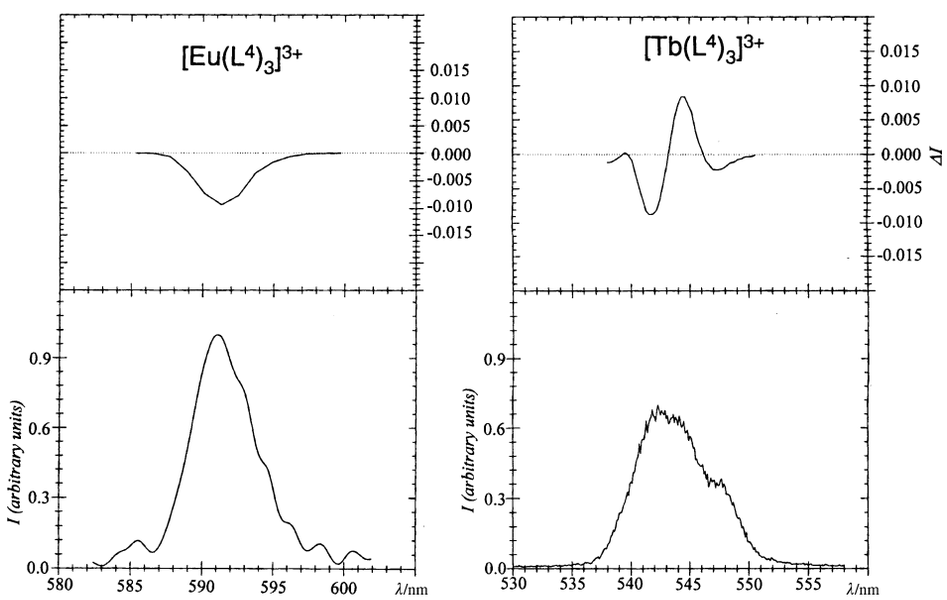

Fig. 2 CPL spectra of $[Ln(L^4)_3]^{3+}$ 10^{-3} M in anhydrous CH_3CN at 298 K, upon excitation at 320 nm. Left: $^5D_0 \longrightarrow {}^7F_1$(Eu) transition, right: $^5D_4 \longrightarrow {}^7F_5$(Tb) transition.

phosphorescence decay is mono-exponential and the corresponding lifetimes amount to 240 ± 2 and 181 ± 5 ms for La and Lu, respectively.

Despite the low intensity metal-centred emission in $[Eu(L^4)_3]^{3+}$ (see Fig. S6†), we have been able to use Eu(III) as a structural probe to investigate the chemical environment of this metal ion in a solid sample of the triple helical complex by high resolution luminescence. At 13 K, the $^5D_0 \longleftarrow {}^7F_0$ excitation spectrum displays one broad and slightly asymmetrical band located at 17211 cm^{-1} with a full width at half height (fwhh) equal to 16.6 cm^{-1}. This band shifts to 17221 cm^{-1} at room temperature while becoming sharper (fwhh = 11.6 cm^{-1}). As a comparison, the same transition has been observed at 17227 cm^{-1} for the corresponding complex with L^1.[11] Using the correlation proposed by Frey and Horrocks[25] relating the energy of the $^5D_0 \longleftarrow {}^7F_0$ transition to the total nephelauxetic effect generated by the ligands bound to the Eu^{III} ion, we predict a value of 17230 cm^{-1} for this transition if the following parameters are taken into account: $\delta_{N(py)} = -16.7$[26] and $\delta_{CO} = -15.7$.[25] The discrepancy is relatively large and may arise from the fact that $\delta_{N(py)}$ has been estimated for polyaminocarboxylates.[26] Moreover, the experimental trend observed in the nephelauxetic effect between the triple helical complexes with L^1 and L^4 is not consistent with the presence of an electron attracting group in the 4-position of the pyridine, which induces less stable 1 : 3 complexes and is expected to produce a somewhat smaller nephelauxetic effect. Nephelauxetic parameters are extremely sensitive to bond lengths and it might well be that the smaller interaction between N(py) and the metal ion in $[Eu(L^4)_3]^{3+}$ causes the Ln–O distances to become longer so that the increased

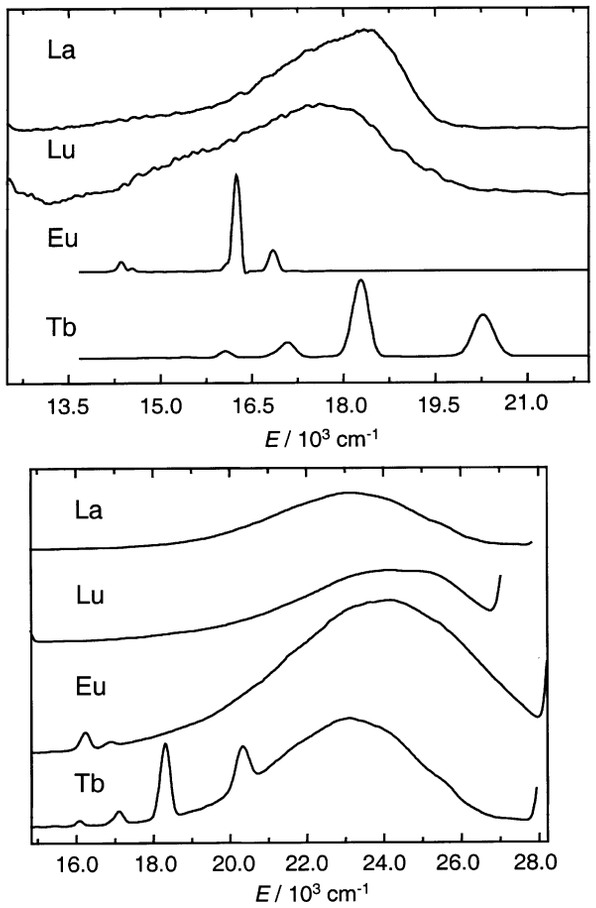

Fig. 3 Top: Time-resolved emission spectra of $[Ln(L^4)_3]^{3+}$ in solid state at 77 K and recorded with time delays of 0.01 (La, Lu) and 0.1 ms (Eu, Tb). Bottom: Emission spectra of $[Ln(L^4)_3]^{3+}$ 10^{-3} M in CH_3CN at 295 K.

nephelauxetic effect of the six carboxamide groups largely overcomes the decreased effect of the three pyridine moieties.

The emission spectrum recorded at 13 K upon excitation through the ligand bands displays relatively broad bands and is typical of a low symmetry environment for the metal ion (Fig. S6 †). The relative intensities of the $^5D_0 \longrightarrow {}^7F_J$ transitions amount to 0.09, 1.00, 6.7, <0.01, and 1.4 for $J = 0$, 1, 2, 3, and 4, respectively. The splitting of the $^7F_1$ level (346, 373 and 428 cm^{-1}) with two relatively close sublevels reflects a symmetry derived from a trigonal arrangement, but more distorted than in $[Eu(L^1)_3]^{3+}$. The $Eu(^5D_0)$ lifetime determined upon broad-band (ligand) or selective ($^5D_0 \longleftarrow {}^7F_0$) excitation decreases from 1.45 ± 0.02 ms between 13 and 77 K to 1.15 ± 0.02 ms at room temperature, pointing to temperature-dependent quenching mechanisms we may trace back to the presence of the fluxional substituent R^1 since this lifetime is somewhat larger (1.8 ms) and temperature-independent in $[Eu(L^1)_3]^{3+}$.[11] Nonetheless, the measured lifetime clearly points to the water molecules evidenced in the elemental analysis and in the vibrational spectrum not being co-ordinated to the metal ion. The lifetime of a 10^{-3} M solution in acetonitrile, 1.58 ± 0.02 ms, also indicates the absence of inner-sphere interaction with water, that is partial decomplexation of one ligand arm through binding of a water molecule does not occur, consistent with the NMR data. The case of the Tb(III) complex is somewhat puzzling in that the lifetime observed in the solid state is quite short, 0.92 ms, but temperature-independent in the range 13–295 K, whilst it is much longer in solution, 1.55 ± 0.01 ms. The latter value is again consistent with no inner-sphere interaction with water while the shorter value in the solid state may arise from self-quenching processes in a closely packed solid.

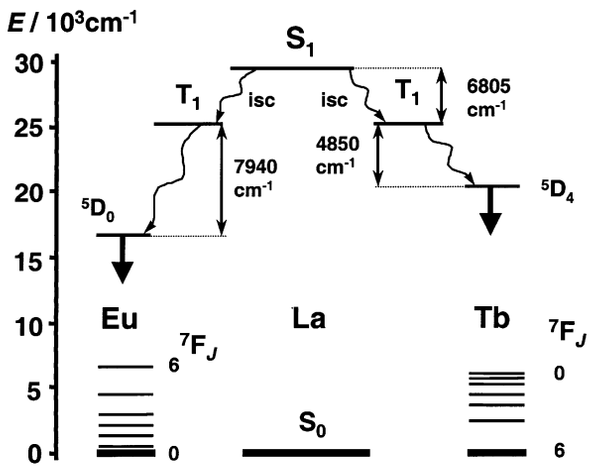

Fig. 4 Schematic energy diagram for $[Ln(L^4)_3]^{3+}$ complexes. Data for S_1 and T_1 are those of the La(III) complex in the solid state at 77 K (0-phonon transitions).

To get a better insight into the various energy conversion processes occurring in the $[Ln(L^4)_3]^{3+}$ complexes, we determined the quantum yields of the ligand- and metal-centred luminescence of 10^{-3} M solutions at 295 K. The ligand itself is essentially non-luminescent and is only weakly luminescent in the complexes with La (Q^F = 0.055%) and Lu (Q^F = 0.065%). The slightly larger quantum yield of the Lu complex with respect to the La complex (factor 1.2) may be explained by a better intersystem crossing (isc) efficiency in the La complex due to a more favourable energy difference: $\Delta E(^1\pi\pi^* - {}^3\pi\pi^*)$ = 6800 cm^{-1} (as determined from the energy of the 0-phonon transitions) as compared to 7545 cm^{-1} for the Lu complex, while it is known that an efficient isc process takes place when $\Delta E(^1\pi\pi^* - {}^3\pi\pi^*)$ is around 5000 cm^{-1}.[27] This in line with the observed decrease in the phosphorescence intensity in going from La to Lu, as exemplified by the ratio $I(^3\pi\pi^*)/I(^1\pi\pi^*)$ which decreases from 8×10^{-3} in $[La(L^4)_3]^{3+}$ to 4.7×10^{-3} in $[Lu(L^4)_3]^{3+}$, that is by a factor 1.7. The quantum yields of the metal-centred luminescence obtained upon ligand excitation are small, $Q^{Ln}{}_L$ = 0.22 and 1.2% for Eu and Tb, respectively. They may be explained by the weak efficiency of the isc process, the emission spectra being dominated by the fluorescence band of the ligand, and by the relative energies of the triplet state of the complexed ligand strands and of the excited $^5D_0$ and $^5D_4$ level (Fig. 4). Indeed, $\Delta E(^3\pi\pi^* - {}^5D_0)$ is very large (almost 8000 cm^{-1}) while $\Delta E(^3\pi\pi^* - {}^5D_4)$, 4850 cm^{-1}, is closer to the ideal value of 2500–3500 cm^{-1} for an efficient ligand-to-metal energy transfer process.[27] With respect to $[Ln(L^1)_3]^{3+}$,[11] the quantum yield for Eu is 26 times larger which reflects the lowering of the ligand triplet state by about 2250 cm^{-1} (as determined from data for the La complexes) induced by the electron-attracting substituent in R^1.

Conclusion

The introduction of a bulky chiral substituent in the pyridine 4-position of L^1 to give L^4 results in a tridentate ligand capable of interacting strongly with trivalent lanthanide ions in acetonitrile resulting in thermodynamically stable 1 : 3 complexes with $\log\beta_3$ in the range 19–20. Compared with complexes with the unsubstituted ligand L^1, the loss of stability due to the introduction of the electron-attracting group in R^1 is relatively small and steric effect seems to be minimum, as indicated by $\Delta\log\beta_3(L^1 - L^4)$ which increases only slightly from La (2.0) to Lu (2.6). In solution, the NMR spectra are consistent with an average pseudo-trigonal symmetry of the $[Ln(L^4)_3]^{3+}$ complexes, but fast P ⇌ M helical interconversion on the NMR time scale prevents diastereomeric segregation in solution.

However, chiro-optical data clearly demonstrate the helical wrapping of the ligand strands around the Ln(III) ions on a shorter time scale, contrary to what was observed when bulky neopentyl substituents were grafted onto the non co-ordinating N atoms of bis(benzimidazole)pyridine to yield L*.[13] Although only a very small excess of one diastereoisomer is induced in solution by the chiral ligand L^4, as shown by CPL data, consequent design of ligands similar to L^4, but producing dynamically inert triple-helical complexes together with a larger diastereomeric induction should lead to luminescent stains able to probe the chirality of more complex molecules, *e.g.* biomolecules, for instance by preferential interaction with one enantiomer. The photophysical properties of the $[Ln(L^4)_3]^{3+}$ complexes can be smoothly rationalised in terms of the energy of the ligand and metal ion excited states and therefore modification of the R^1 substituent leading to a better antenna effect should be within reach.

Experimental

Solvents and starting materials

Acetonitrile, dichloromethane, chloroform, tetrahydrofuran, diethyl ether and petroleum ether were purified in the usual way.[28] Silica gel (Merk 60, 0.04–0.06 mm) was used for preparative column chromatography. Other products were purchased from Fluka AG (Buchs, Switzerland) or Merck and used without further purification. Lanthanide perchlorates were obtained as previously described.[29] **CAUTION**: dry perchlorates and their complexes with aromatic amines may easily explode and should be handled in small quantities and with extreme caution.[30]

Spectroscopic and analytical measurements

Electronic spectra in the UV-vis range were recorded at 293 K with a Perkin-Elmer Lambda 900 spectrometer using 1.0 and 0.1 cm quartz cells. Reflectance spectra were recorded as finely ground powders dispersed in MgO (5%), with MgO as the reference, on the same spectrometer equipped with a Labsphere PELA-1000 integration sphere. Specific rotary dispersion values were measured from 10^{-3} M solutions in degassed anhydrous acetonitrile at 298 K with the help of a JASCO DIP-370 polarimeter (sodium D line). IR spectra were obtained from KBr pellets with a Mattson α-Centauri FT-IR spectrometer. Pneumatically-assisted electrospray (ES-MS) mass spectra were recorded from CH_3CN solutions on API III or API 3000 tandem mass spectrometers (PE Sciex) by infusion at 10 μl min^{-1}. The spectra were recorded under low up-front declustering or collision induced dissociation (CID) conditions, typically ΔV = 0–30 V between the orifice and the first quadrupole of the spectrometer. ^{1}H and ^{13}C-NMR spectra were recorded at 25 °C on Bruker AM-360 or Bruker AVANCE 400-DRX spectrometers. Chemical shifts are reported in parts per million with respect to TMS. Ligand excitation and emission spectra were recorded on a Perkin-Elmer LS-50B spectrometer equipped for low temperature (77 K) measurements. The experimental procedures for high resolution laser excited luminescence studies have been published previously.[31] Emission spectra were corrected for the instrumental function. Quantum yields of the ligand-centred emission were measured relative to quinine sulfate in 0.05 M H_2SO_4 (A_{347} = 0.05, absolute quantum yield: 0.546).[32] Quantum yields of the metal-centred emission were determined as previously described[33] at excitation wavelengths where (i) the Lambert–Beer law is obeyed and (ii) the absorption of the reference $[Ln(terpy)_3]^{3+}$ closely matches that of the sample. Elemental analyses were performed by Dr H. Eder (Microchemical Laboratory, University of Geneva).

Spectrophotometric titrations

The electronic spectra in the UV-vis range were recorded at 298 K from 10^{-4} M solutions in acetonitrile (spectroscopy grade) containing Et_4NClO_4 0.1 M as inert electrolyte with a Perkin-Elmer Lambda 7 spectrometer connected to an external computer and using quartz cells of 0.1 cm path length. Solutions were prepared in a thermostatted vessel (Metrohm 6.1418.220) and the titrant solution was added with an automated burette from Metrohm (6.1569.150 or .210) fitted with an anti-diffusion device. In a typical experiment, 5–10 mL of L^4 were titrated with a solution of Ln(III) triflate 10^{-4} M in acetonitrile. After each addition of 0.20 mL and a delay of 2 min, the spectrum was measured and transferred to the computer. In some instances, reverse titrations, *i.e.* with L^4 as titrating species, were also performed to confirm the values of the stability constants. All the experiments were conducted in a dry box and the water content of the solutions, measured at the end of the titration by the Karl Fischer method, was always <30 ppm. Factor analysis and stability constant determinations were carried out with the program SPECFIT, version 2.10.[34]

Preparation of the ligand (Scheme 2)

4-Bromopyridine-2,6-dicarbonyl dibromide (1). PBr_3 (9.3 cm^3, 98.9 mmol) was added slowly to a vigorously stirred solution of bromine (4.2 cm^3, 81.9 mmol) in petroleum ether (35 cm^3). The solvent was removed *in vacuo* after complete precipitation of PBr_5. Chelidamic acid (5 g, 27.3 mmol) was added and the reaction mixture was heated to 90 °C under reflux for 4 h. The residue was cooled to rt and extracted three times with $CHCl_3$ (75 cm^3). The combined organic layers were concentrated. The residue was purified by Kugelrohr distillation (160–185 °C/0.5 mmHg) to give 8.8 g of **1** (21.8 mmol, 80%) as a white solid. ^{1}H-NMR (400 MHz) in $CDCl_3$: δ 8.38 (2H, s). ^{13}C-NMR (100 MHz) in $CDCl_3$: δ 130.78, 135.90, 150.54, 166.74. IR ν (cm^{-1}, KBr): 1763, 1246, 908.

4-Bromo-*N*,*N*,*N*′,*N*′-tetraethylpyridine-2,6-dicarboxamide (2). 1 (2.2 g, 5.9 mmol) was dissolved in diethyl ether (50 cm^3) followed by the addition of diethylamide (2.5 cm^3, 23.9 mmol) at 0 °C. After stirring at 0 °C for ten minutes the reaction mixture was stirred at rt for 20 min. The solvent was removed *in vacuo* and the residue was crystallised from acetylacetate to give 1.7 g of **2** (4.8 mmol, 81%) as a colourless solid. Mp 92–94 °C. ^{1}H-NMR (400 MHz) in $CDCl_3$: δ 1.17 (6 H, t, ^3J = 7.2 Hz), 1.27 (6 H, t, ^3J = 7.2 Hz), 3.34 (4 H, q, ^3J = 7.2 Hz), 3.56 (4 H, q, ^3J = 7.2 Hz), 7.81 (2 H, s). ^{13}C-NMR (100 MHz) in $CDCl_3$: δ 12.72, 14.24, 40.27, 43.27, 127.10, 134.53, 154.50, 166.70. IR ν(cm^{-1}, KBr): 1628, 1564, 1460, 1444. MS (FAB, 70 eV) *m*/*z*: 356, 358 (M + 1).

3-[2,6-Bis(diethylcarbamoyl)pyridine-4-yl]-*N*-(*tert*-butoxycarbonyl)alanine methyl ester (L^4). Two 10 cm^3 round-bottom flasks were dried, one of them charged with zinc (216.6 mg, 3.31 mmol). Dibromoethane (0.016 cm^3, 0.23 eq) was added under inert atmosphere and warmed to 60 °C for 3 min. Tetrahydrofuran (3 cm^3) and trimethylsilyl chloride (5 cm^3, 0.05 eq) were added after cooling the dibromethane mixture to 30 °C and stirred for 30 min, prior to heating to 60 °C and addition of iodoalanine (326.8 mg, 0.993 mmol). Stirring was continued until complete consumption of iodoalanine as judged by thin layer chromatography. The second flask was loaded with **2** (295 mg, 0.828 mmol) and $(Ph_3P)_2PdCl_2$ (30.7 mg, 0.044 mmol) under argon. The zinc reagent (**3**) was transferred with a syringe into the second flask and the mixture was warmed to 50 °C and stirred for 24 h. Evaporation of the solvent left a brown oil which was purified by flash chromatography (SiO_2, diethyl ether : petroleum ether 2 : 1) to give 377 mg of L^4 (0.788 mmol, 95%) as a colourless solid. Mp 87–90 °C. [Found: C, 60.0; H, 8.0; N 11.4. Calc. for $C_{24}H_{38}O_6N_4$: C, 60.2; H, 8.0; N, 11.7%]. ^{1}H-NMR (400 MHz) in CD_3CN: δ 1.07 (6 H, t, ^3J = 7.15 Hz), 1.19 (6 H, t, ^3J = 7.15 Hz), 1.34 (9 H, s), 3.00 (1 H, m), 3.22 (1 H,

m), 3.23 (4 H, q, ^3J = 7.15 Hz), 3.49 (4 H, q, ^3J = 7.15 Hz), 3.68 (3 H, s), 4.46 (1 H, m), 5.70 (1 H, d, ^3J = 8.3 Hz), 7.35 (2 H, s). ^{13}C-NMR (400 MHz) in CD_3CN: δ 12.14, 13.59, 27.44, 36.45, 39.48, 42.85, 51.97, 53.82, 123.20, 149.05, 154.31, 167.77, 171.80. IR ν(cm^{-1}, KBr): 1744, 1712, 1628. MS *m*/*z*: 478 (M^+, 16%), 351 (M − Boc − $C_2H_2^+$, 100%).

Preparation of the complexes

The 1 : 3 complexes $[Ln(L^4)_3](ClO_4)_3 \cdot solv$ (Ln = La, *solv* = 0, **4**; Eu, *solv* = 2.5 H_2O, **5**; Tb, *solv* = 3 H_2O, 1 CH_3CN, **6**; Lu, *solv* = 0, **7**) were prepared by mixing L^4 with stoichiometric amounts of $Ln(ClO_4)_3 \cdot nH_2O$ (Ln = La, Eu, Tb, Lu and n = 0.2–0.6) in dichloromethane–acetonitrile. The complexes could be directly isolated in 70–80% yield by removing the solvent. The slow diffusion of a solvent in which the complexes are not soluble, led to the formation of oils. **4**; Found: C, 46.0; H, 6.3; N, 9.0. Calc. for $C_{72}H_{114}N_{12}O_{30}Cl_3La$: C, 46.2; H, 6.1; N, 9.0%. **5**; Found: C, 44.8; H, 6.2; N, 8.7. Calc. for $C_{72}H_{114}N_{12}O_{30}Cl_3Eu \cdot 2.5H_2O$: C, 44.8; H, 6.2; N, 8.7%. **6**; Found: C, 44.7; H, 6.2; N, 9.2. Calc. for $C_{72}H_{114}N_{12}O_{30}Cl_3Tb \cdot 3H_2O \cdot CH_3CN$: C, 44.7; H, 6.3; N, 9.2%. **7**; Found: C, 45.3; H, 6.0; N, 8.9. Calc. for $C_{72}H_{114}N_{12}O_{30}Cl_3Lu$: C, 45.3; H, 6.0; N, 8.8%. IR ν(cm^{-1}, KBr): 1599 (La), 1601 (Eu), 1602 (Tb), 1606 (Lu) (ν_{CO}); 1089, 625 (ionic ClO_4^-).

Acknowledgements

This work is supported through grants from the Swiss National Science Foundation. We thank Véronique Foiret for her help in recording the high resolution luminescence spectra, Dennis Ehlert for improving the ligand synthesis, Paula Gawryszewska for measuring the CPL spectra, Prof. Pierre Vogel for the use of his polarimeter and the Fondation Herbette (Lausanne) for the gift of spectroscopic equipment.

References

1 D. Parker, *Coord. Chem. Rev.*, 2000, **205**, 109.
2 V. W. W. Yam and K. K. W. Lo, *Coord. Chem. Rev.*, 1999, **184**, 157.
3 Z. J. Guo and P. J. Sadler, *Angew. Chem., Intl. Ed.*, 1999, **38**, 1513.
4 J.-C. G. Bünzli, in *Rare Earths*, ed. R. Saez Puche and P. Caro, Editorial Complutense, Madrid, 1998, pp. 223–259.
5 C. Piguet and J.-C. G. Bünzli, *Chem. Soc. Rev.*, 1999, **28**, 347.
6 C. Piguet, C. Edder, H. Nozary, F. Renaud, S. Rigault and J.-C. G. Bünzli, *J. Alloys Compd.*, 2000, **303/304**, 94.
7 C. Piguet, C. Edder, S. Rigault, G. Bernardinelli, J.-C. G. Bünzli and G. Hopfgartner, *J. Chem. Soc., Dalton Trans.*, 2000, 3999.
8 J.-M. Bénech, C. Piguet, G. Bernardinelli, J.-C. G. Bünzli and G. Hopfgartner, *J. Chem. Soc., Dalton Trans.*, 2001, 684; H. Nozary, C. Piguet, J.-P. Rivera, P. Tissot, G. Bernardinelli, N. Vulliermet, J. Weber and J.-C. G. Bünzli, *Inorg. Chem.*, 2000, **39**, 5286.
9 E. Huskowska and J. P. Riehl, *Inorg. Chem.*, 1995, **34**, 5615.
10 F. Renaud, C. Piguet, G. Bernardinelli, J.-C. G. Bünzli and G. Hopfgartner, *Chem. Eur. J.*, 1997, **3**, 1660.
11 F. Renaud, C. Piguet, G. Bernardinelli, J.-C. G. Bünzli and G. Hopfgartner, *Chem. Eur. J.*, 1997, **3**, 1646.
12 G. Muller, PhD Dissertation, University of Lausanne, 2000.
13 G. Muller, J.-C. G. Bünzli, K. J. Schenk, C. Piguet and G. Hopfgartner, *Inorg. Chem.*, 2001, **40**, 2642.
14 R. F. W. Jackson, N. Wishart, A. Wood, K. James and M. Wythes, *J. Org. Chem.*, 1992, **57**, 3397.
15 S. Gair, R. F. W. Jackson and P. A. Brown, *Tetrahedron Lett.*, 1997, **38**, 3059.
16 J. M. Fox, X. H. Huang, A. Chieffi and S. L. Buchwald, *J. Am. Chem. Soc.*, 2000, **122**, 1360.
17 H. Takalo, P. Pasanen and J. Kankare, *Acta Chem. Scand. Ser. B*, 1987, **41**, 219.
18 H. Takalo, P. Pasanen and J. Kankare, *Acta Chem. Scand. Ser. B*, 1988, **42**, 373.
19 J. A. Bajgrowicz, A. El Hallaoui, R. Jacquier, C. Pigiere and P. Viallefont, *Tetrahedron Lett.*, 1985, **41**, 1833.
20 S. AchyuthaRao and P. Knochel, *J. Org. Chem.*, 1991, **56**, 4591.
21 M. J. Dewar, E. V. Zoebisch, E. F. Healy and J. J. P. Stewart, *J. Am. Chem. Soc.*, 1985, **107**, 3902.
22 W. Zarges, J. Hall, J.-M. Lehn and C. Bolm, *Helv. Chim. Acta*, 1991, **74**, 1843.
23 N. Coruh, G. L. Hilmes and J. P. Riehl, *Inorg. Chem.*, 1988, **27**, 3647.
24 J. P. Riehl and F. S. Richardson, *Chem. Rev.*, 1986, **86**, 1.
25 S. T. Frey and W. deW. Horrocks Jr., *Inorg. Chim. Acta*, 1995, **229**, 383.
26 M. Latva and J. Kankare, *J. Coord. Chem.*, 1998, **43**, 121.
27 F. J. Steemers, W. Verboom, D. N. Reinhoudt, E. B. Vandertol and J. W. Verhoeven, *J. Am. Chem. Soc.*, 1995, **117**, 9408.
28 D. D. Perrin and W. L. F. Armarego, *Purification of Laboratory Chemicals*, Pergamon Press, Oxford, 1988.
29 J.-C. G. Bünzli, J.-R. Yersin and C. Mabillard, *Inorg. Chem.*, 1982, **21**, 1471.
30 W. C. Wolsey, *J. Chem. Educ.*, 1973, **50**, A335.
31 N. Martin, J.-C. G. Bünzli, V. McKee, C. Piguet and G. Hopfgartner, *Inorg. Chem.*, 1998, **37**, 577.
32 S. R. Meech and D. C. Phillips, *J. Photochem.*, 1983, **23**, 193.
33 H.-R. Mürner, E. Chassat, R. P. Thummel and J.-C. G. Bünzli, *J. Chem. Soc., Dalton Trans.*, 2000, 2809.
34 H. Gampp, M. Maeder, C. J. Meyer and A. D. Zuberbühler, *Talanta*, 1985, **23**, 1133.